Annals of Communications in Mathematics

Volume 8, Number 2 (2025), 275-292 DOI: 10.62072/acm.2025.080210

ISSN: 2582-0818

https://www.technoskypub.com/journal/acm/



SINE TYPE II TOPP-LEONE GOMPERTZ DISTRIBUTION WITH APPLICATIONS

SULE OMEIZA BASHIRU* AND THATAYAONE MOAKOFI

ABSTRACT. Probability distributions are essential for modeling and analyzing complex datasets across various scientific disciplines. However, classical distributions often fail to capture intricate features such as skewness, heavy tails, or high variability observed in real-world data. To address these limitations, this study proposes the Sine Type II Topp-Leone Gompertz (STIITLG) distribution, a novel extension of the Gompertz model based on the sine type II Topp-Leone family. The proposed model enhances the flexibility of the classical Gompertz distribution by incorporating an additional shape parameter, enabling it to better accommodate diverse data behaviors. Several key properties of the model, including moments, inverse moment, mean residual life function, entropy, and order statistics, were derived to establish its theoretical foundation. The model parameters were estimated using the maximum likelihood estimation method, and a comprehensive simulation study confirmed the consistency of these estimators. The practical utility of the model was demonstrated by applying it to two real-life datasets, where it outperformed several existing models based on goodness-of-fit criteria. These findings underscore the potential of the proposed distribution as a robust tool for modeling complex phenomena in diverse fields.

1. Introduction

Probability distributions are fundamental tools in statistics and applied mathematics, playing a crucial role in modeling and analyzing data across various fields such as engineering, finance, healthcare, environmental science, and reliability studies. By providing a mathematical framework to describe the likelihood of different outcomes, these distributions facilitate decision-making processes and enable practitioners to predict, simulate, and understand complex systems. From risk assessment in insurance to survival analysis in medical research, probability distributions are indispensable for addressing real-world challenges.

²⁰²⁰ Mathematics Subject Classification. 62G20, 65C60.

Key words and phrases. Sine type II Topp-Leone generator; Gompertz distribution; moments; maximum likelihood estimation method; simulation; real life data.

Received: May 20, 2025. Accepted: June 20, 2025. Published: June 30, 2025.

Copyright © 2025 by the Author(s). Licensee Techno Sky Publications. This article is an open-access article distributed under the terms and conditions of the Creative Commons Attribution (CC BY) license (https://creativecommons.org/licenses/by/4.0/).

^{*}Corresponding author.

However, classical probability distributions often face limitations in capturing the complexities of modern datasets. These challenges stem from the inherent simplicity of traditional models, which are typically characterized by fixed hazard rate shapes, limited skewness, and inflexibility in describing high variability. As data becomes increasingly intricate such as in fields dealing with heterogeneous populations, catastrophic events, or rapidly evolving phenomena, the need for extended or compounded distributions becomes evident. These extensions address the constraints of classical models by providing enhanced flexibility and improved fit to real-world data.

A particularly effective method for extending classical models is the use of generalized families of distributions, often referred to as generators. These generators introduce additional parameters, such as scale or shape parameters, into existing distributions, thereby increasing their flexibility. Recent examples include the new Lomax generator by [17], Ristić Balakrishnan Topp–Leone Gompertz generator by [28], Harris-Topp-Leone generator by [29], tangent exponential generator by [27], DUS Topp-Leone generator by [11], exponent power sine generator by [32], Marshall–Olkin exponentiated half logistic generalized-G by [31], extended Modi generator by [30], and cosine inverse Lomax-G by [33].

The Gompertz distribution, introduced as a model for human mortality rates, is widely recognized for its applications in demography, reliability engineering, and survival analysis. Its exponential-like form makes it particularly suitable for modeling increasing hazard rates, which are common in aging processes and systems experiencing wear and tear. Despite its usefulness, the Gompertz distribution has limitations when applied to datasets with more complex structures, such as those exhibiting high variability or heavy-tailed behavior.

To address these limitations, researchers have developed extensions of the Gompertz distribution (GD) by incorporating additional parameters or compounding it with other distribution families. Some notable variants of the Gompertz distribution include the type I half logistic GD by [25], odd Lindley GD by [18], power GD by [20], Lomax GD by [21], alpha power GD by [15], Marshall-Olkin GD by [24], extended GD by [12], Topp-Leone GD by [19], exponentiated generalized extended GD by [16], cosine GD by [34], and new modified GD by [13].

In this study, the Gompertz distribution is extended using the sine type II Topp-Leone family of distributions, a versatile framework known for its ability to introduce an additional shape parameter and capture a wide range of data behaviors. The sine type II Topp-Leone family has demonstrated significant potential in enhancing the flexibility of baseline distributions, making it a suitable choice for this purpose. By compounding the Gompertz distribution with this family, we introduce the sine type II Topp-Leone Gompertz (STIITLG) distribution, a new model designed to overcome the limitations of the classical Gompertz distribution while retaining its interpretability and practical relevance.

The primary objective of this research is to develop a new compound distribution that not only generalizes the Gompertz distribution but also provides a better fit to complex datasets encountered in various fields. This study derives the mathematical properties of the proposed distribution, estimates its parameters using the maximum likelihood estimation method, and evaluates its performance using real-life datasets. The findings are expected to demonstrate the advantages of this extension, offering a robust tool for researchers and practitioners dealing with sophisticated modeling challenges.

The structure of this study is as follows: Section 2 outlines the construction of the STIITLG model and presents its reliability measures. Section 3 details the linear expansion

of the model's probability density function (PDF) and cumulative distribution function (CDF). Statistical properties are derived in Section 4, while Section 5 describes the parameter estimation method. The results of the simulation study are provided in Section 6. Application results are given in Section 7. Finally, concluding remarks are presented in Section 8.

2. PROPOSED MODEL FORMULATION

The cumulative distribution function (CDF) of the sine type II Topp-Leone generator as proposed by [1] is given as:

$$F(x) = \sin\left\{\frac{\pi}{2} \left[1 - \left(1 - (G(x))^2\right)^{\kappa}\right]\right\}$$
 (2.1)

and the corresponding probability density function (PDF) is given as

$$f(x) = \frac{\pi}{2} 2\kappa g(x)G(x) \left[1 - (G(x))^2 \right]^{\kappa - 1} \cos \left\{ \frac{\pi}{2} \left[1 - \left(1 - (G(x))^2 \right)^{\kappa} \right] \right\}; x > 0, \tag{2.2}$$

where $\kappa > 0$ is a shape parameter, g(x) and G(x) denote the PDF and CDF of a baseline distribution, respectively.

The PDF and CDF of the Gompertz distribution are given in Equations (2.3) and (2.4).

$$g(x) = \tau e^{\delta x} e^{-\frac{\tau}{\delta} \left(e^{\delta x} - 1\right)},\tag{2.3}$$

$$G(x) = 1 - e^{-\frac{\tau}{\delta}(e^{\delta x} - 1)},$$
 (2.4)

where $\tau > 0$ is the shape parameter and $\delta > 0$ is a scale parameter.

By substituting Equation (2.4) into Equation (2.1), the CDF of the STIITLG distribution is obtained as:

$$F(x) = \sin\left\{\frac{\pi}{2} \left[1 - \left(1 - \left(1 - e^{-\frac{\tau}{\delta}(e^{\delta x} - 1)}\right)^2\right)^{\kappa}\right]\right\}.$$
 (2.5)

The corresponding PDF is obtained by substituting Equations (2.3) and (2.4) into Equation (2.2), and is given as:

$$f(x) = \frac{\pi}{2} 2\kappa \left(\tau e^{\delta x} e^{-\frac{\tau}{\delta} \left(e^{\delta x} - 1 \right)} \right) \left(1 - e^{-\frac{\tau}{\delta} \left(e^{\delta x} - 1 \right)} \right)$$

$$\times \left[1 - \left(1 - e^{-\frac{\tau}{\delta} \left(e^{\delta x} - 1 \right)} \right)^2 \right]^{\kappa - 1} \cos \left\{ \frac{\pi}{2} \left[1 - \left(1 - \left(1 - e^{-\frac{\tau}{\delta} \left(e^{\delta x} - 1 \right)} \right)^2 \right)^{\kappa} \right] \right\}, \tag{2.6}$$

for $\kappa, \tau, \delta > 0$, and $x \ge 0$.

The PDF and CDF plots of the STIITLG model are given in figure 1. From the PDF plot it can be seen that the proposed model is right skewed. The CDF plot, ranging from 0 to 1, confirms that the model is properly defined, as it satisfies the fundamental property of a cumulative distribution function by being non-decreasing and bounded between 0 and 1.

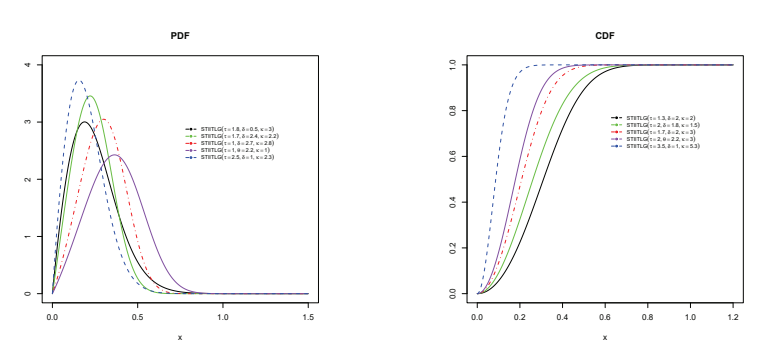


FIGURE 1. PDF and CDF Plots of the STIITLG distribution

2.1. **Reliability Measures.** The survival function (SF) gives the probability that a system or component will function beyond a certain time x. The survival function of the STIITLG distribution is defined as:

$$s(\mathbf{x}) = 1 - \sin\left\{\frac{\pi}{2} \left[1 - \left(1 - \left(1 - e^{-\frac{\tau}{\delta}(e^{\delta x} - 1)}\right)^2\right)^{\kappa}\right]\right\}. \tag{2.7}$$

The hazard rate function (hrf), also known as the failure rate function, describes the instantaneous likelihood of an event occurring at a given time x, given that it has not yet occurred. The hrf of the STIITLG distribution is given by:

$$h(x) = \frac{\frac{\pi}{2} \cdot 2\kappa \left(\tau e^{\delta x} e^{-\frac{\tau}{\delta}(e^{\delta x} - 1)}\right) \left(1 - e^{-\frac{\tau}{\delta}(e^{\delta x} - 1)}\right) \left[1 - \left(1 - e^{-\frac{\tau}{\delta}(e^{\delta x} - 1)}\right)^{2}\right]^{\kappa - 1}}{1 - \sin\left\{\frac{\pi}{2}\left[1 - \left(1 - \left(1 - e^{-\frac{\tau}{\delta}(e^{\delta x} - 1)}\right)^{2}\right)^{\kappa}\right]\right\}} \times \cos\left\{\frac{\pi}{2}\left[1 - \left(1 - \left(1 - e^{-\frac{\tau}{\delta}(e^{\delta x} - 1)}\right)^{2}\right)^{\kappa}\right]\right\}.$$
(2.8)

The SF and hrf plots of the proposed model are shown in Figure 2. The SF decreases over time, as expected, indicating the diminishing probability of survival. The hrf exhibits a monotonically increasing pattern.

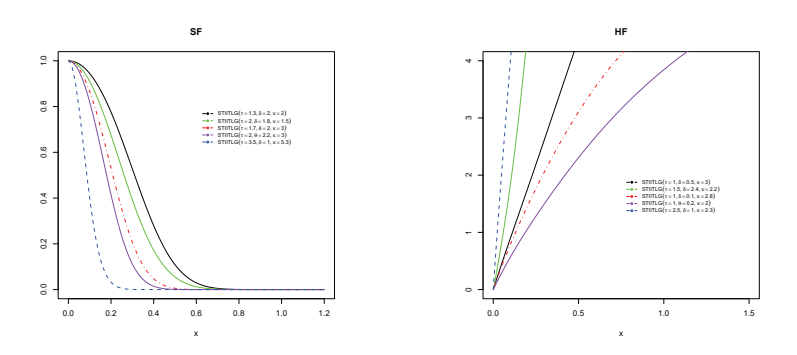


FIGURE 2. Survival and hazard function plots of the STIITLG distribution

The cumulative hazard function (CHF) that follows the STIITLG model is given as:

$$CHF(x) = -\log\left(1 - \sin\left\{\frac{\pi}{2}\left[1 - \left(1 - \left(1 - e^{-\frac{\tau}{\delta}\left(e^{\delta x} - 1\right)}\right)^2\right)^{\kappa}\right]\right\}\right).$$

3. LINEAR EXPANSION

In this section, we utilize an expansion technique to reformulate the density functions in equations (2.5) and (2.6), making them more accessible for analysis and the derivation of statistical properties. By employing a suitable series expansion, we express the CDF and PDF in a more computationally convenient form.

The CDF in Equation (2.5) above can be expanded using Taylor's series expression as follows:

$$F(x) = \sin\left\{\frac{\pi}{2}\left[1 - \left(1 - \left(1 - e^{-\frac{\tau}{\delta}\left(e^{\delta x} - 1\right)}\right)^{2}\right)^{\kappa}\right]\right\}$$

$$= \sum_{i=0}^{\infty} \frac{(-1)^{i}}{(2i+1)!} \frac{\pi^{2i+1}}{2^{2i+1}} \left(1 - \left(1 - \left(1 - e^{-\frac{\tau}{\delta}\left(e^{\delta x} - 1\right)}\right)^{2}\right)^{\kappa}\right)^{2i+1}.$$
(3.1)

The last part of Equation (3.1) can be expanded using binomial expansion as follows:

$$\left(1 - \left(1 - e^{-\frac{\tau}{\delta}(e^{\delta x} - 1)}\right)^{2}\right)^{\kappa}\right)^{2i+1} = \sum_{j=0}^{\infty} (-1)^{j} \binom{2i+1}{j} \left(1 - \left(1 - e^{-\frac{\tau}{\delta}(e^{\delta x} - 1)}\right)^{2}\right)^{\kappa j},$$

$$\left(1 - \left(1 - e^{-\frac{\tau}{\delta}(e^{\delta x} - 1)}\right)^{2}\right)^{\kappa j} = \sum_{l=0}^{\infty} (-1)^{l} \binom{kj}{l} \left(1 - e^{-\frac{\tau}{\delta}(e^{\delta x} - 1)}\right)^{2l},$$

$$\left(1 - e^{-\frac{\tau}{\delta}(e^{\delta x} - 1)}\right)^{2l} = \sum_{m=0}^{\infty} (-1)^{m} \binom{2l}{m} e^{-\frac{m\tau}{\delta}(e^{\delta x} - 1)},$$

$$e^{-\frac{m\tau}{\delta}(e^{\delta x} - 1)} = \sum_{n=0}^{\infty} \left(-\frac{m\tau}{\delta}\right)^{n} \frac{1}{n!} (e^{\delta x} - 1)^{n},$$

$$\left(e^{\delta x} - 1\right)^{n} = \sum_{p=0}^{\infty} (-1)^{n+p} \binom{n}{p} e^{\delta xp}.$$

Hence the CDF in Equation (2.5), can be written as:

$$F(x) = \sum_{i,j,l,m,n,p=0}^{\infty} \frac{(-1)^{i+j+l+m+n+p}}{(2i+1)!\kappa!} \frac{\pi^{2i+1}}{2^{2i+1}} {2i+1 \choose j} {kj \choose l} {2l \choose m} \left(-\frac{mt}{\delta}\right)^n {n \choose p} e^{\delta xp}$$

$$= \sum_{i,j,l,m,n,p=0}^{\infty} \psi e^{\delta xp},$$
(3.2)

where

$$\psi = \frac{(-1)^{i+j+l+m+n+p}}{(2i+1)!\kappa!} \frac{\pi^{2i+1}}{2^{2i+1}} \left(\begin{array}{c} 2i+1 \\ j \end{array} \right) \left(\begin{array}{c} kj \\ l \end{array} \right) \left(\begin{array}{c} 2l \\ m \end{array} \right) \left(-\frac{mt}{\delta} \right)^n \left(\begin{array}{c} n \\ p \end{array} \right).$$

By considering the last part of the PDF (2.6), we have

$$\cos\left\{\frac{\pi}{2}\left[1-\left(1-\left(1-e^{-\frac{\tau}{\delta}\left(e^{\delta x}-1\right)}\right)^{2}\right)^{\kappa}\right]\right\} = \sum_{q=0}^{\infty} \frac{(-1)^{q}}{(2q)!} \frac{\pi^{2q}}{2^{2q}} \left[1-\left(1-\left(1-e^{-\frac{\tau}{\delta}\left(e^{\delta x}-1\right)}\right)^{2}\right)^{\kappa}\right]^{2q}.$$
(3.3)

The last term in Equation (3.3) can be expanded using binomial expansion as follows:

$$\left[1 - \left(1 - \left(1 - e^{-\frac{\tau}{\delta}(e^{\delta x} - 1)}\right)^{2}\right)^{\kappa}\right]^{2q} = \sum_{s=0}^{\infty} (-1)^{s} {2q \choose s} \left(1 - \left(1 - e^{-\frac{\tau}{\delta}(e^{\delta x} - 1)}\right)^{2}\right)^{\kappa s},$$

$$\left(1 - \left(1 - e^{-\frac{\tau}{\delta}(e^{\delta x} - 1)}\right)^{2}\right)^{\kappa s + \kappa - 1} = \sum_{t=0}^{\infty} (-1)^{t} {\kappa s + \kappa - 1 \choose t} \left(1 - e^{-\frac{\tau}{\delta}(e^{\delta x} - 1)}\right)^{2t},$$

$$\left(1 - e^{-\frac{\tau}{\delta}(e^{\delta x} - 1)}\right)^{2t+1} = \sum_{u=0}^{\infty} (-1)^{u} {2t+1 \choose u} e^{-\frac{u\tau}{\delta}(e^{\delta x} - 1)},$$

$$e^{-\frac{ut}{\delta}(e^{\delta x} - 1)(u+1)} = \sum_{v=0}^{\infty} \left(\frac{-ut(u+1)}{\delta}\right)^{v} \frac{1}{v!} (e^{\delta x} - 1)^{v},$$

$$\left(e^{\delta x} - 1\right)^{v} = \sum_{w=0}^{\infty} (-1)^{v+w} {v \choose w} e^{\delta xw}.$$

The PDF in (2.6) can be written as:

$$\begin{split} f(x) &= \sum_{q,s,t,u,v,w=0}^{\infty} \frac{(-1)^{q+s+t+u+v+w} 2\kappa}{(2q)!v!} \frac{\pi^{2q+1}}{2^{2q+1}} \binom{2q}{s} \binom{ks+k+1}{t} \binom{2t+1}{u} \binom{v}{w} \\ &\times \left(\frac{-ut(u+1)}{\delta}\right)^{v} e^{\delta x(w+1)} \\ &= \sum_{q,s,t,u,v,w=0}^{\infty} \varphi \, e^{\delta x(w+1)}, \end{split} \tag{3.4}$$

where

$$\varphi = \frac{\left(-1\right)^{q+s+t+u+v+w}2\kappa}{\left(2q\right)!v!} \frac{\pi^{2q+1}}{2^{2q+1}} \left(\begin{array}{c} 2q \\ s \end{array}\right) \left(\begin{array}{c} \kappa s + \kappa + 1 \\ t \end{array}\right) \left(\begin{array}{c} 2t + 1 \\ u \end{array}\right) \left(\begin{array}{c} v \\ w \end{array}\right) \left(\frac{-ut\left(u+1\right)}{\delta}\right)^v.$$

4. STATISTICAL PROPERTIES

Several statistical properties of the proposed distribution are presented in this section.

4.1. **Quantile Function.** The quantile function, defined as the inverse of the cumulative distribution function (CDF), plays a crucial role in statistical analysis. It provides a direct way to generate random samples from a distribution and facilitates the computation of various statistical measures, including percentiles and interquartile ranges. For more

insights, see [26]. The quantile function of the proposed model is given by:

$$Q(F) = \frac{\ln\left\{1 - \frac{\delta}{\tau} \left(\ln\left(1 - \left(1 - \left(1 - \frac{\sin^{-1}(u)}{\frac{\pi}{2}}\right)^{1/\kappa}\right)^{1/2}\right)\right)\right\}}{\delta}.$$
 (4.1)

4.2. **Moments.** Moments are fundamental statistical measures that provide insights into the shape, central tendency, and variability of a probability distribution. The r^{th} moment of the proposed model is given as:

$$\mu'_{r} = \int_{-\infty}^{\infty} x^{r} f(x) dx = \sum_{q,s,t,u,v,w=0}^{\infty} \varphi \int_{0}^{\infty} x^{r} e^{\delta x(w+1)} dx = \sum_{q,s,t,u,v,w=0}^{\infty} \varphi \frac{\Gamma(r+1)}{\left[-(\delta(w+1))\right]^{r+1}}.$$
(4.2)

By setting r = 1, 2, 4 and 4 in Equation (4.2), the first four moments can be expressed as:

$$\begin{split} \mu_1' &= \sum_{q,s,t,u,v,w=0}^{\infty} \varphi \frac{\Gamma(2)}{\left[-(\delta(w+1))\right]^2}, \\ \mu_2' &= \sum_{q,s,t,u,v,w=0}^{\infty} \varphi \frac{\Gamma(3)}{\left[-(\delta(w+1))\right]^3}, \\ \mu_3' &= \sum_{q,s,t,u,v,w=0}^{\infty} \varphi \frac{\Gamma(4)}{\left[-(\delta(w+1))\right]^4}, \\ \mu_4' &= \sum_{q,s,t,u,v,w=0}^{\infty} \varphi \frac{\Gamma(5)}{\left[-(\delta(w+1))\right]^5}. \end{split}$$

The skewness (S_k) and kurtosis (K_u) of the proposed model are given by:

$$S_k = \frac{\mu_3' - 3\mu\mu_2' + 2\mu^3}{(\mu_2' - \mu^2)^{3/2}},$$

$$K_u = \frac{\mu_4' - 4\mu\mu_3' + 6\mu^2\mu_2' - 3\mu^4}{(\mu_2' - \mu^2)^2}.$$

Figure 3 presents the skewness and kurtosis plots of the STIITLG distribution. It is evident that, for a fixed value of δ , both skewness and kurtosis increase as κ and τ vary. A similar pattern is observed when τ is fixed and κ and δ vary.

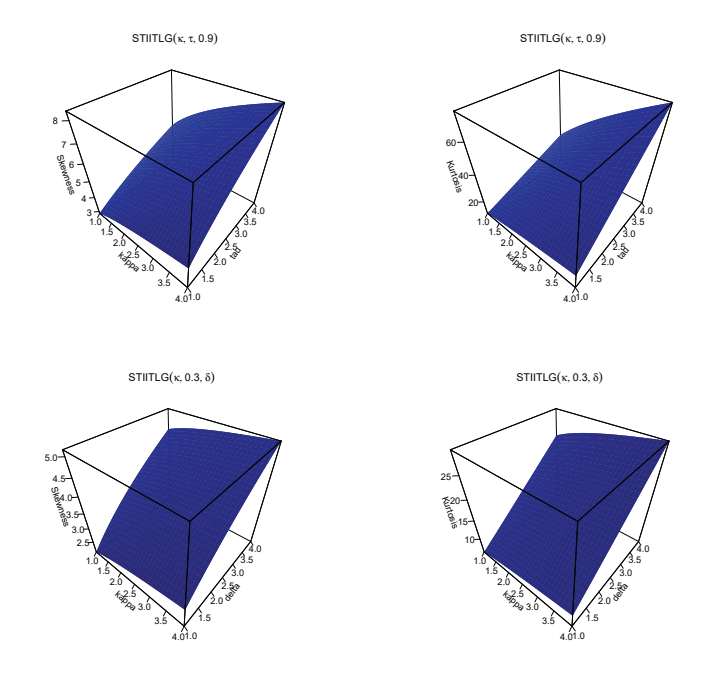


FIGURE 3. 3D plots of skewness and kurtosis for the STIITLG distribution

4.3. **Inverse Moments.** Inverse moments provide insights into the expected values of the reciprocal of a random variable, which are particularly useful in reliability analysis and risk assessment. The inverse moment of the proposed model is given by:

$$\mu'_{-r} = \int_{-\infty}^{\infty} x^{-r} f(x) dx = \sum_{q,s,t,v,w=0}^{\infty} \varphi \int_{0}^{\infty} x^{-r} e^{\delta x(w+1)} dx$$
$$= \sum_{q,s,t,u,v,w=0}^{\infty} \varphi (-(\delta(w+1)))^{r-1} \Gamma(1-r).$$

4.4. **Mean Residual Life Function.** The mean residual life (MRL) function quantifies the expected remaining lifetime of a system or component, given that it has survived up to a specific time. It plays a crucial role in reliability analysis, maintenance planning, and replacement strategies. For the proposed distribution, the MRL function is given by:

$$\begin{split} MRLF(m) &= \frac{1}{S(m)} \int\limits_{m}^{\infty} x f(x) dx - m = \frac{1}{S(m)} \sum_{q,s,t,u,v,w=0}^{\infty} \varphi \int\limits_{m}^{\infty} x e^{\delta x(w+1)} dx - m, \\ &= \frac{1}{S(m)} \sum_{q,s,t,u,v,w=0}^{\infty} \varphi \frac{e^{\delta (w+1)m} (\delta (w+1)m-1)}{\delta^2 (w+1)^2} - m, \end{split}$$

where S(m) is the survival function of the STIITLG distribution.

4.5. **Mean Inactive Time function.** The mean inactivity time (MIT) function provides a measure of the expected time a system or component has been inactive before a specified

time point. It is a crucial reliability metric used to analyze failure patterns and predict system behavior. The MIT function has diverse applications in reliability theory, survival analysis, biomedical research, and actuarial science. For the STIITLG model, the MIT function is given by:

$$MIT = p - \frac{1}{F(p)} \int_{0}^{p} x f(x) dx = p - \frac{1}{F(p)} \sum_{q,s,t,u,v,w=0}^{\infty} \varphi \int_{0}^{p} x e^{\delta x(w+1)} dx,$$
$$= p - \frac{1}{F(p)} \sum_{q,s,t,u,v,w=0}^{\infty} \varphi \frac{e^{\delta p(w+1)} (\delta p(w+1) - 1) + 1}{\delta^{2}(w+1)^{2}},$$

where F(p) is the CDF of the STIITLG distribution.

4.6. **Entropy.** Entropy measures the uncertainty or randomness associated with a probability distribution, providing insights into the amount of information required to describe a random variable. Rényi entropy, a generalized form of Shannon entropy, is widely applied in various fields. The Rényi entropy of the proposed model is given by:

$$R.E_{\lambda}(x) = \frac{1}{1-\lambda} \log \int_0^{\infty} f(x)^{\lambda} dx = \frac{1}{1-\lambda} \log \int_0^{\infty} \left(\sum_{q,s,t,u,v,w=0}^{\infty} \varphi e^{\delta x(w+1)} \right)^{\lambda} dx.$$

4.7. **Order Statistics.** Suppose that x_1, x_2, \ldots, x_n are n random samples from the STIITLG model, which has the CDF in (3.2) and the PDF in (3.4). Let $x_{(1)}, x_{(2)}, \ldots, x_{(n)}$ be the observed order statistics. The PDF of the k^{th} order statistic is computed as follows:

$$f_{X_{(k)}}(x) = \frac{n!}{(k-1)!(n-k)!} f(x; \gamma, \omega, \alpha) [F(x; \gamma, \omega, \alpha)]^{k-1} [1 - F(x; \gamma, \omega, \alpha)]^{n-k}.$$
(4.3)

Substituting equations (3.2) and (3.4) into equation (4.3), we obtain the PDF of the k^{th} order statistic for the STIITLG model as follows:

$$f_{X_{(k)}}(x) = \frac{n!}{(k-1)!(n-k)!} \left(\sum_{q,s,t,u,v,w=0}^{\infty} \varphi e^{\delta x(w+1)} \right) \left[\sum_{i,j,l,m,n,p=0}^{\infty} \psi e^{\delta xp} \right]^{k-1} \times \left[1 - \sum_{i,j,l,m,n,p=0}^{\infty} \psi e^{\delta xp} \right]^{n-k} . \tag{4.4}$$

5. METHOD OF ESTIMATION

This section presents the approach used to estimate the parameters of the STIITLG model.

5.1. **Maximum Likelihood Estimation Method.** Let $X_1, X_2...X_n$ be a random sample from the STIITLG distribution, and let $x_1, x_2...x_n$ denote to the observed values of the

sample. In this case, the log-likelihood function is given by:

$$\ell(\tau, \delta, \kappa) = \ln\left(\frac{\pi}{2}\right) + \ln 2 + \ln \kappa + \ln \tau + \delta \sum_{i=1}^{n} x_i - \frac{\tau}{\delta} \sum_{i=1}^{n} \left(e^{\delta x_i} - 1\right) + \sum_{i=1}^{n} \ln\left(1 - e^{-\frac{\tau}{\delta}\left(e^{\delta x_i} - 1\right)}\right) + (\kappa - 1) \sum_{i=1}^{n} \ln\left(1 - \left(1 - e^{-\frac{\tau}{\delta}\left(e^{\delta x_i} - 1\right)}\right)^2\right) + \sum_{i=1}^{n} \ln\cos\left\{\frac{\pi}{2}\left[1 - \left(1 - \left(1 - e^{-\frac{\tau}{\delta}\left(e^{\delta x_i} - 1\right)}\right)^2\right)^{\kappa}\right]\right\}.$$
 (5.1)

To obtain the maximum likelihood estimates (MLEs) of the parameters τ , δ and κ , we differentiate the log-likelihood function with respect to each parameter and set the resulting score equations to zero:

$$\frac{\partial \ell}{\partial \tau} = 0, \quad \frac{\partial \ell}{\partial \delta} = 0, \quad \frac{\partial \ell}{\partial \kappa} = 0.$$

These nonlinear equations generally do not have closed-form solutions; therefore, numerical methods such as the Newton-Raphson algorithm or expectation-maximization (EM) algorithm are employed to obtain the estimates.

6. SIMULATION

With the maximum likelihood estimation (MLE) method discussed in Section 5, the performance of the STIITLG distribution is examined by conducting various simulations for different sizes (n=25, 50, 100, 200, 400, 800, 1200) via the R package. We simulate N=3000 samples for the true parameters values of (κ, τ, δ) given in Table 1 and Table 2. These tables report the mean estimates, average bias (ABIAS), and root mean squared errors (RMSEs) of the MLEs across different sample sizes. The ABIAS and RMSE for an estimated parameter, say $\hat{\kappa}$, are computed as follows:

$$ABIAS(\hat{\kappa}) = \frac{\sum_{i=1}^{N} \hat{\kappa}_i}{N} - \kappa, \quad \text{and} \quad RMSE(\hat{\kappa}) = \sqrt{\frac{\sum_{i=1}^{N} (\hat{\kappa}_i - \kappa)^2}{N}},$$

respectively.

TABLE 1. Monte Carlo Simulation Results

TABLE 1. Monte Cario Simulation Results											
		((0.2, 0.8, 0	.2)	(0.8, 0.2, 0.8)						
Parameter	Sample Size	Mean	RMSE	ABIAS	Mean	RMSE	ABIAS				
κ	25	0.8551	0.4782	0.6551	0.6027	0.5503	-0.1972				
	50	0.7168	0.3865	0.5168	0.6327	0.4952	-0.1672				
	100	0.5361	0.3217	0.3361	0.6418	0.4480	-0.1581				
	200	0.5067	0.2683	0.3067	0.6475	0.4107	-0.1524				
	400	0.3354	0.2045	0.1354	0.6652	0.3487	-0.1347				
	800	0.2421	0.1473	0.0621	0.6978	0.2852	-0.1021				
	1200	0.2380	0.1261	0.0380	0.7194	0.2421	-0.0805				
au	25	1.1002	0.5950	0.3002	0.4905	0.4809	0.2905				
	50	0.9889	0.4797	0.1889	0.3517	0.2292	0.1517				
	100	0.9019	0.4172	0.1019	0.3202	0.2909	0.1202				
	200	0.7278	0.3239	-0.0721	0.3188	0.2150	0.1188				
	400	0.8479	0.2923	0.0479	0.3019	0.1982	0.1019				
	800	0.8409	0.2391	0.0409	0.2589	0.1466	0.0589				
	1200	0.7855	0.2004	-0.0144	0.2284	0.1293	0.0284				
δ	25	0.2938	0.1168	-0.0938	0.6149	0.3533	-0.1850				
	50	0.1100	0.1065	-0.0899	0.6653	0.3017	-0.1346				
	100	0.1326	0.0862	-0.0673	0.6747	0.2594	-0.1252				
	200	0.1296	0.0884	-0.0703	0.6769	0.2330	-0.1230				
	400	0.1584	0.0626	-0.0415	0.6904	0.1954	-0.1095				
	800	0.1733	0.0422	-0.0266	0.7132	0.1573	-0.0868				
	1200	0.1829	0.0400	-0.0171	0.7391	0.1244	-0.0608				

TARIF 2	Monte	Carlo	Simulation	Results
IADLE 4.	MIUHIC	Carro	Dimuiauvii	IXCSUIG

TABLE 2. Wionte Carlo Simulation Results											
		(0	.6, 0.6, 0.	6)	(1.2, 0.6, 1.2)						
Parameter	Sample Size	Mean	RMSE	ABIAS	Mean	RMSE	ABIAS				
κ	25	0.7255	0.6932	0.1255	1.3107	0.5433	0.1107				
	50	0.6803	0.6498	0.0803	1.2742	0.4459	0.0742				
	100	0.6646	0.5577	0.0646	1.2509	0.3713	0.0509				
	200	0.6540	0.5196	0.0540	1.2385	0.3161	0.0385				
	400	0.6487	0.4577	0.0487	1.2380	0.2823	0.0380				
	800	0.6377	0.3844	0.0377	1.2244	0.2492	0.0244				
	1200	0.6207	0.3325	0.0207	1.2144	0.2378	0.0144				
au	25	0.6753	0.3962	0.0753	0.7750	0.6576	0.1750				
	50	0.6696	0.3233	-0.0696	0.7313	0.5919	0.1313				
	100	0.6574	0.2901	-0.0574	0.7175	0.4923	0.1175				
	200	0.64728	0.2581	-0.0471	0.7123	0.4524	0.1123				
	400	0.5612	0.2301	-0.0387	0.6862	0.3925	0.0862				
	800	0.5751	0.2021	-0.0248	0.6790	0.3567	0.0790				
	1200	0.5968	0.1769	-0.0031	0.6698	0.3224	0.0698				
δ	25	1.0852	0.8630	0.4852	1.6126	1.0657	0.4126				
	50	0.8381	0.6479	0.2381	1.3561	0.8579	0.1561				
	100	0.7778	0.5787	0.1778	1.2807	0.7688	0.0807				
	200	0.7567	0.5058	0.1567	1.2682	0.6996	0.0682				
	400	0.6855	0.4473	0.0855	1.2284	0.6377	0.0284				
	800	0.6363	0.3780	0.0363	1.2262	0.5567	0.0262				
	1200	0.6017	0.3331	0.0017	1.1938	0.5059	-0.0061				

The results in Tables 1 and 2 indicate that as the sample size (n) increases, the mean estimates of the parameters converge towards the true values. Additionally, both ABIAS and RMSE decrease towards zero, highlighting the stability of the STIITLG distribution.

7. APPLICATIONS

In this section, we illustrate the performance of the STIITLG distribution by fitting it to two real data sets. We compared the STIITLG distribution with several other non-nested models, namely Topp-Leone inverse Gompertz (TLIG) by [2], generalized Weibull (GW) by [4], Type I Half Logistic-Weibull (TIHL-W) by [6], alpha power Weibull (APW) distribution by [5], generalized Weibull-Gompertz (GWGom) distribution by [3] and Harris extended Gompertz (HEGom) distribution by [8]. The pdfs of these distributions are given as follows:

$$f_{TIHL-W}(x;\lambda,\delta,\gamma) = \frac{2\lambda\delta\gamma x^{\gamma-1}e^{-\lambda\delta x^{\gamma}}}{[1+e^{-\lambda\delta x^{\gamma}}]^2},$$

for $\lambda, \delta, \gamma > 0$ and x > 0,

$$f_{TLIG}(x; \alpha, \lambda, \beta) = 2\alpha \lambda x^{-2} \exp\left(\frac{\beta}{x}\right) \exp\left(\frac{-\lambda}{\beta} \exp\left(\frac{\beta}{x} - 1\right)\right) \times \left[1 - \exp\left(\frac{-\lambda}{\beta} \exp\left(\frac{\beta}{x} - 1\right)\right)\right] \times \left(1 - \left[1 - \exp\left(\frac{-\lambda}{\beta} \exp\left(\frac{\beta}{x} - 1\right)\right)\right]^{2}\right)^{\alpha - 1},$$

for $\alpha, \lambda, \beta > 0$, and x > 0,

$$f_{GW}(x; w, \lambda, \gamma) = w\lambda \gamma x^{\lambda - 1} \left(1 + \gamma x^{\lambda} \right)^{w - 1} \exp\left(1 - \left(1 + \gamma x^{\lambda} \right)^{w} \right),$$
 for $w, \lambda, \gamma > 0$, and $x > 0$,

$$f_{APW}(x;\alpha,\beta,\lambda) = \frac{\lambda\beta\alpha^{1-\exp(-\lambda x^{\beta})}\exp(-\lambda x^{\beta})x^{\beta-1}\log(\alpha)}{\alpha-1},$$
 for $\alpha,\beta,\lambda>0$, and $x>0$

for $\alpha, \beta, \lambda > 0$, and x > 0

$$f_{GWGom}(x;a,b,c,d) = abx^{b-1} \exp\left(-ax^b \left[\exp(cx^d) - 1\right] + cx^d\right) \left(1 + \left(\frac{cd}{b}\right)x^d - \exp(-cx^d)\right)$$
 for $a,b,c,d > 0$, and $x > 0$, and

$$f_{HEGom}(x;\theta,k,\beta,c) = \theta^{1/k}\beta c^x \exp\left(-\beta \frac{c^x - 1}{\log(c)}\right) \left[\left(1 - (1 - \theta) \exp\left(-k\beta \frac{c^x - 1}{\log(c)}\right)\right)^{1 + \frac{1}{k}}\right]^{-1}$$
 for $\theta,k,\beta,c > 0$, and $x > 0$.

The performance of the models were assessed using the well recognized goodness-of-fit statistics, namely, -2loglikelihood (-2 log (L)), Akaike Information Criterion (AIC), Consistent Akaike Information Criterion (CAIC), Bayesian Information Criterion (BIC), Cramer-Von Mises (W^*) and Andersen-Darling (A^*) as described by Chen and Balakrishnan [10]. We also computed the Kolmogorov-Smirnov (K-S) goodness-of-fit statistic. The model with the smallest values of these goodness-of-fit statistics and a higher p-value for the K-S statistic, is regarded as the best fitting model.

We present plots of fitted densities, histograms of the data, and probability plots for each example to show how well our model fits the observed data sets. To obtain the probability plot, we plotted $F_{STIITLG}(x_{(j)};\hat{\kappa},\hat{\tau},\hat{\delta})$ against $\frac{j-0.375}{n+0.25},\,j=1,\,2,\,\cdots,\,n,$ where $x_{(j)}$ are the ordered values of the observed data. The measures of closeness are given by the sum of squares $SS = \sum_{j=1}^{n} \left[F_{STIITLG}(x_{(j)}; \hat{\kappa}, \hat{\tau}, \hat{\delta}) - \left(\frac{j - 0.375}{n + 0.25} \right) \right]^2$.

7.1. Waiting Times data. The dataset presented below contains the waiting times (in minutes) before service for 100 bank customers. It was recently used by [9] and [14]. The data are as follows:

$$0.8, 0.8, 1.3, 1.5, 1.8, 1.9, 1.9, 2.1, 2.6, 2.7, 2.9, 3.1, 3.2, 3.3, 3.5, 3.6, 4.0, 4.1, 4.2, \\4.2, 4.3, 4.3, 4.4, 4.4, 4.6, 4.7, 4.7, 4.8, 4.9, 4.9, 5.0, 5.3, 5.5, 5.7, 5.7, 6.1, 6.2, 6.2, \\6.2, 6.3, 6.7, 6.9, 7.1, 7.1, 7.1, 7.1, 7.4, 7.6, 7.7, 8.0, 8.2, 8.6, 8.6, 8.6, 8.8, 8.8, 8.9, 8.9, \\$$

 $9.5, 9.6, 9.7, 9.8, 10.7, 10.9, 11.0, 11.0, 11.1, 11.2, 11.2, 11.5, 11.9, 12.4, 12.5, 12.9, \\13.0, 13.1, 13.3, 13.6, 13.7, 13.9, 14.1, 15.4, 15.4, 17.3, 17.3, 18.1, 18.2, 18.4, 18.9, \\19.0, 19.9, 20.6, 21.3, 21.4, 21.9, 23.0, 27.0, 31.6, 33.1, 38.5.$

TABLE 3. Parameter Estimates and Goodness-of-Fit Statistics for Various Models Fitted to the Waiting Times Data

	Estimates				Statistics							
Model	κ	τ	δ		$-2 \log L$	AIC	AICC	BIC	W^*	A^*	K-S	p-value
STIITLG	0.7036	0.1258	2.2961×10 ⁻⁰⁹		635.2183	641.2184	641.4684	649.0339	0.0322	0.2072	0.0629	0.8224
	(0.3154)	(0.0355)	(0.0120)									
	λ	δ	γ									
TIHLW	1.6402×10^{-04}	1.4636×10^{03}	8.0447×10^{-01}		663.5575	669.5578	669.8078	677.3733	0.0355	0.2263	0.190	0.0013
	(3.1919×10^{-05})	(6.8591×10^{-09})	(6.9384×10^{-02})									
	α	λ	β									
TLIG	4.1166×10^{-01}	1.6168×10^{01}	4.4063×10^{-08}		654.3819	660.3819	660.6319	668.1974	0.2256	1.5436	0.0915	0.3722
	(1.8900×10^{-01})	(6.0799)	(2.5275×10^{-02})									
	w	λ	γ									
GW	0.2442	3.3820	0.0062		644.5253	650.5253	650.7753	658.3408	0.0482	0.3332	0.0934	0.3466
	(0.0704)	(0.5547)	(0.0026)									
	α	β	γ									
APW	1.0647×10^{11}	5.1064×10^{-01}	1.3453		649.9905	655.9901	656.2401	663.8056	0.0645	0.4694	0.1369	0.0469
	(5.8543×10^{-14})	(3.8749×10^{-02})	(1.1917×10^{-01})									
	a	b	c	d								
GWGom	1.4738×10^{02}	5.7825×10^{-01}	5.3742×10^{-04}	5.1797×10^{-01}	649.782	657.7825	658.2035	668.2032	0.0327	0.2129	0.1438	0.0318
	(5.7146×10^{-07})	(4.4948×10^{-02})	(1.3538×10^{-04})	(4.5057×10^{-02})								
	θ	k	β	c								
HEGom	1.6033	0.0261	0.1181	1.0383	648.107	656.107	656.5281	666.5277	0.1201	0.7576	0.1130	0.1555
	(2.0870)	(0.1072)	(0.1692)	(0.0279)								

Table 3 presents the maximum likelihood estimates (MLEs) of the fitted distributions, along with their standard errors (in parentheses) and the corresponding goodness-of-fit statistics. Based on the results in Table 3, the STIITLG distribution demonstrated the best fit for the waiting times data set among the competing models. This conclusion is supported by the goodness-of-fit measures: $AIC, AICC, BIC, W^*, A^*$, and K-S, which yielded the lowest values for the STIITLG distribution. Additionally, the STIITLG distribution exhibited the highest p-value among the fitted models, further distinguishing it from the alternatives.

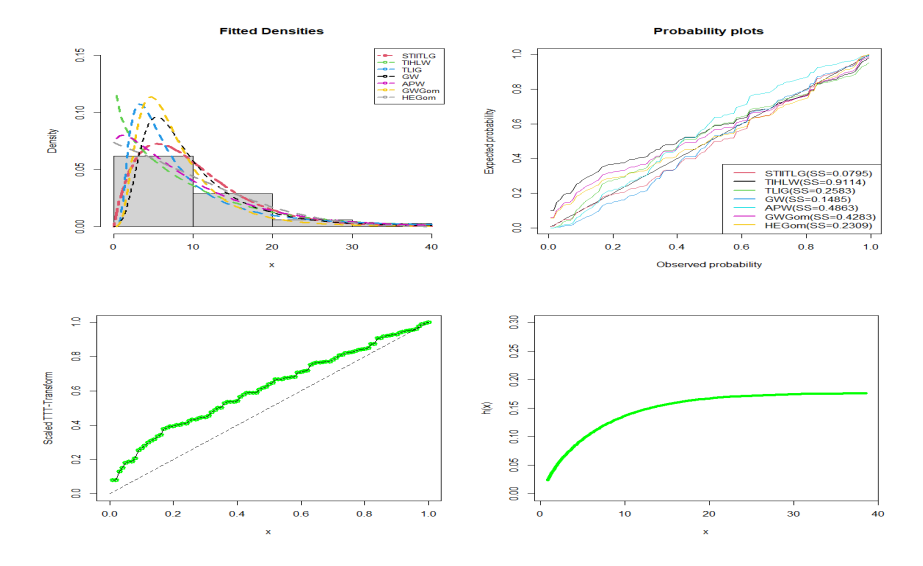


FIGURE 4. Fitted densities, probability plots, fitted hazard rate function (hrf) and Scaled TTT-Transform plots for the STIITLG distribution for waiting times data

Figure 4 presents the fitted density plots, probability plots, total time on test (TTT) plot, and hazard rate function (hrf) plot. These visualizations indicate that the STIITLG distribution provided a better fit to the data compared to other models. The hrf follows an increasing pattern in the TTT scaled plot. Furthermore, the estimated hrf of the STIITLG distribution exhibits an increasing trend, reinforcing its compatibility with the waiting times data set.

7.2. **Carbon Fibres data.** The second dataset consists of the breaking stress values (in GPa) for carbon fibres with a length of 50 mm. These data were previously analyzed by [7], [22], and [23]. The observed values are as follows:

 $0.39, 0.85, 1.08, 1.25, 1.47, 1.57, 1.61, 1.61, 1.69, 1.80, 1.84, 1.87, 1.89, 2.03, 2.03, \\ 2.05, 2.12, 2.35, 2.41, 2.43, 2.48, 2.50, 2.53, 2.55, 2.55, 2.56, 2.59, 2.67, 2.73, 2.74, \\ 2.79, 2.81, 2.82, 2.85, 2.87, 2.88, 2.93, 2.95, 2.96, 2.97, 3.09, 3.11, 3.11, 3.15, 3.15, \\ 3.19, 3.22, 3.22, 3.27, 3.28, 3.31, 3.31, 3.33, 3.39, 3.39, 3.56, 3.60, 3.65, 3.68, 3.70, \\ 3.75, 4.20, 4.38, 4.42, 4.70, 4.90.$

TABLE 4. Parameter Estimates and Goodness-of-Fit Statistics for Various Models Fitted to the Carbon Fibres Data

various violets i fitted to the Carbon i fores Data												
			Statistics									
Model	κ	τ	δ		$-2 \log L$	AIC	AICC	BIC	W^*	A^*	K-S	p-value
STIITLG	25.3631	0.0255	0.4101		171.9248	177.9247	178.3118	184.4937	0.0749	0.4976	0.0923	0.6274
	(1.1437×10^{-04})	(4.5335×10^{-03})	(7.6808×10^{-02})									
	λ	δ	γ									
TIHLW	1.1246e+03	1.0494×10^{-04}	2.3155		176.3865	182.3869	182.774	188.9558	0.0879	0.4917	0.1511	0.0982
	(9.8332×10^{-13})	(1.0555×10^{-05})	(1.3372×10^{-09})									
	α	λ	β									
TLIG	5.1971	1.1596	$2.0020e \times 10^{-08}$		231.1911	237.1911	237.5782	243.7601	0.7532	4.2460	0.2413	0.0009
	(3.8634)	(0.5372)	(2.8649×10^{-02})									
	w	λ	γ									
GW	0.9636	3.2014	0.0312		172.9805	178.9805	179.3676	185.5494	0.1007	0.5577	0.1202	0.2958
	(0.4724)	(0.5215)	(0.0190)									
	α	β	γ									
APW	1.0647×10^{-10}	0.8638	1.5559		192.6593	198.6593	199.0464	205.2282	0.3806	2.0867	0.1290	0.2216
	(6.5424×10^{-14})	(0.0826)	(0.1398)									
	a	b	c	d								
GWGom	1.8531×10^{02}	6.3266×10^{-05}	9.1732×10^{-04}	1.6862	210.6949	218.6958	219.3516	227.4545	0.1772	0.9487	0.2553	0.0004
	(2.7248×10^{-06})	(0.0940)	(2.2593×10^{-04})	(0.0950)								
	θ	k	β	c								
HEGom	1.1856	5.3098	0.0409	2.8481	175.4249	183.4249	184.0806	192.1835	0.1015	0.7295	0.1090	0.4122
	(0.6844)	(10.8392)	(0.0223)	(0.4653)								

Based on the results in Table 4, the STIITLG distribution demonstrates the best fit among the competing distributions. This conclusion is supported by its lowest values for $-2\ln(L)$, AIC, CAIC, BIC, W^* , A^* , and the K-S statistic. Additionally, the p-value associated with the K-S statistic is the highest for the STIITLG distribution, further indicating that this distribution provides the most suitable fit for the carbon fibres data.

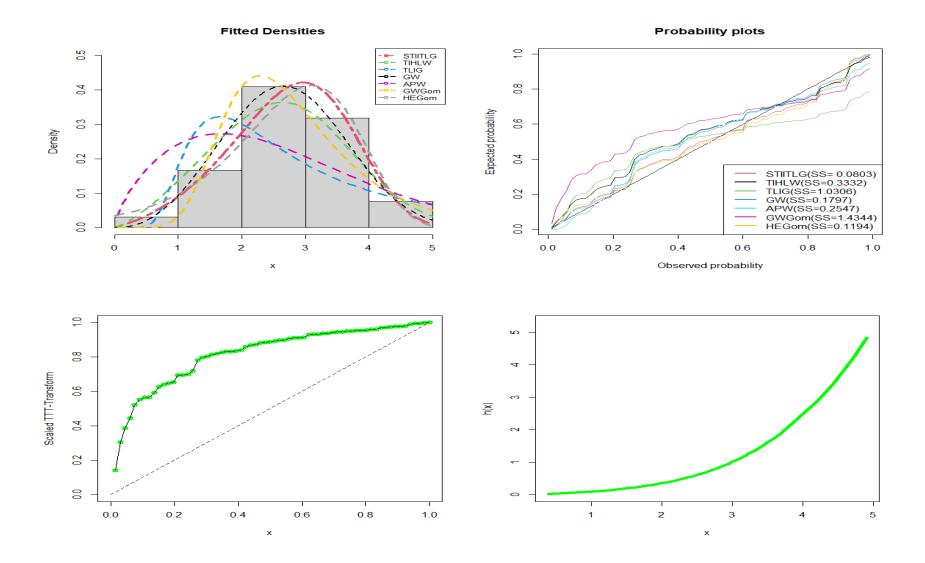


FIGURE 5. Fitted densities and PP plots, fitted hazard rate function and Scaled TTT-Transform plots for the STIITLG distribution for carbon fibres data

For the second dataset, Figure 5 illustrates the fitted density and probability plots, along with the TTT and hrf plots. The STIITLG distribution emerges as the best fit as shown by the fitted density and probability plots. The hrf follows an increasing trend in the TTT plot. The estimated hrf further supports its suitability for modeling the data.

8. CONCLUDING REMARKS

This study introduced a novel extension of the Gompertz distribution by incorporating the sine type II Topp-Leone family of distributions, adding an additional shape parameter to enhance the flexibility of the classical model. Several important properties of the proposed distribution, including moments, the moment-generating function, and order statistics, were derived to establish its theoretical foundation. The parameters of the model were estimated using the maximum likelihood estimation method, and a simulation study confirmed the consistency and reliability of these estimators. The practical utility of the proposed model was demonstrated through its application to two real-life datasets, where it exhibited superior performance compared to several existing models. The findings of this study underscore the potential of the proposed model as a robust and versatile tool for analyzing complex datasets. Future research could focus on exploring additional applications of the model in fields such as economics, survival analysis, and environmental studies, as well as investigating alternative parameter estimation techniques and extensions involving other generator families.

9. ACKNOWLEDGEMENTS

The authors would like to thank the anonymous reviewers for their valuable comments and suggestions.

REFERENCES

- A. M. Isa, S. I. Doguwa, B. B. Alhaji, and H. G. Dikko. Sine type II Topp-Leone-G family of probability distribution: mathematical properties and application, Arid Zone Journal of Basic and Applied Research, 2(4)(2023), 124–138.
- [2] T. M. Adegoke, O. M. Oladoja, S. O. Bashiru, A. A. Mustapha, D. E. Aderupatan and L. C. Nzei. Topp-Leone inverse Gompertz distribution: properties and different estimations techniques and applications, Pakistan Journal of Statistics, 39(4)(2023),433–456.
- [3] A. H. El-Bassiouny, M. El-Damcese, A. Mustafa and M. S. Eliwa. Exponentiated generalized Weibull-Gompertz distribution with application in survival analysis, Journal of Statistics Applications & Probability, 6(1)(2017), 7–16.
- [4] T. Dimitrakopoulou, K. Adamidis and S. Loukas. A lifetime distribution with an upside-down bathtub-shaped hazard function, IEEE Transactions on Reliability, 56(2)(2007), 308–311.
- [5] M. Nassar, A. Alzaatreh, M. Mead and O. Abo-Kasem. Alpha power Weibull distribution: properties and applications, Communications in Statistics-Theory and Methods, 46(20)(2017), 10236–10252.
- [6] D. Kumar, N. Jain and S. Gupta. The type I generalized half-logistic distribution based on upper record values, Journal of Probability and Statistics, 2015(1)(2015), 393608.
- [7] S. Aliyu and M. A. Bamanga. Estimation and comparison of Weibull-normal distribution with some other probability models using Bayesian method of estimation, Science World Journal, 19(1)(2024), 92–100.
- [8] A. Batsidis and A. J. Lemonte. On the Harris extended family of distributions, Statistics, 49(6)(2015), 1400–1421.
- [9] B. Oluyede, T. Moakofi, F. Chipepa and B. Makubate. A new power generalized Weibull-G family of distributions: properties and applications, Journal of Statistical Modelling: Theory and Applications, 1(2)(2020), 167–191.
- [10] G. Chen and N. Balakrishnan. A general purpose approximate goodness-of-fit test, Journal of Quality Technology, 27(2)(1995), 154–161.
- [11] D.-F. N. Ekemezie, K. E. Anyiam, M. Kayid, O. S. Balogun and O. J. Obulezi. DUS Topp—Leone-G family of distributions: baseline extension, properties, estimation, simulation and useful applications, Entropy, 26(973)(2024).
- [12] M. S. Eliwa, M. Masoom Ali, A. El-Gohary, R. El-Desokey, Mohamed Ibrahim, and M. El-Morshedy. Extended Gompertz distribution: properties and estimation under complete and censored data, Journal of Statistics Applications & Probability, 11(3)(2022), 1107–1121.
- [13] E. A. Debelu and A. T. Goshu. New modified Gompertz probability distribution with flexible hazard functions, Journal of Probability and Statistics, 2024(2024), Article ID 7420260, 20 pages.
- [14] S. O. Bashiru, I. Ali, A. M. Auwal, and A. M. Isa. Sine type II Topp-Leone exponential distribution: properties, simulation and application, Confluence University Journal of Science and Technology, 1(2)(2024),126–137. doi:10.5455/CUJOSTECH.241008.
- [15] J. T. Eghwerido, L. C. Nzei, and F. I. Agu. The alpha power Gompertz distribution: characterization, properties, and applications, Sankhya A, 83(2021), 449–475.
- [16] T A. N. De Andrade, S. Chakraborty, L. Handique, and F. Gomes-Silva. The exponentiated generalized extended Gompertz distribution, Journal of Data Science, 17(2)(2022), 299–330.
- [17] L. P. Sapkota, V. Kumar, A. M. Gemeay, M. E. Bakr, O. S. Balogun, and A. H. Muse. New Lomax-G family of distributions: statistical properties and applications, AIP Advances, 13(9)(2023), 095128.
- [18] S. Kuje, K. E. Lasisi, S. C. Nwaosu, and A. M. A. Alkafawi. On the properties and applications of the odd Lindley-Gompertz distribution, Asian Journal of Science and Technology, 10(10)(2019), 10364–10370.
- [19] L. C. Nzei, J. T. Eghwerido, and N. Ekhosuehi. Topp-Leone Gompertz distribution: properties and applications, Journal of Data Science, 18(4)(2022), 782–794.
- [20] T. G. Ieren, F. M. Kromtit, B. U. Agbor, I. B. Eraikhuemen, and P. O. Koleoso. A power Gompertz distribution: model, properties and application to bladder cancer data, Asian Research Journal of Mathematics, 15(2)(2019), 1–14.
- [21] A. Omale, O. E. Asiribo, and A. Yahaya. On properties and applications of Lomax-Gompertz distribution, Asian Journal of Probability and Statistics, 3(2)(2019), 1–17.
- [22] S. O. Bashiru and I. I. Itopa. Modeling of reliability and survival data with exponentiated generalized inverse Lomax distribution, Reliability: Theory & Applications, 4(76)(2023), 493–501. doi:10.24412/1932-2321-2023-476-493-501.
- [23] S. O. Bashiru. A new extended generalized inverse exponential distribution: properties and applications, Asian Journal of Probability and Statistics, 11(2)(2021), 30–46. doi:10.9734/ajpas/2021/v11i230264.

- [24] J. T. Eghwerido, J. O. Ogbo, and A. E. Omotoye. The Marshall-Olkin Gompertz distribution: properties and applications, Statistica, 81(2)(2021), 183–215.
- [25] A. A. Ogunde, O. I. Oseghale, and A. T. Audu. Performance rating of the type I half logistic Gompertz distribution: an analytical approach, American Journal of Mathematics and Statistics, 7(3)(2017), 93–98.
- [26] S. O. Bashiru, M. Kayid, R. M. Sayed, O. S. Balogun, M. M. Abd El-Raouf, and A. M. Gemeay. Introducing the unit Zeghdoudi distribution as a novel statistical model for analyzing proportional data, Journal of Radiation Research and Applied Sciences, 18(1)(2025), 101204. doi:10.1016/j.jrras.2024.101204.
- [27] E. Hussam, L. P. Sapkota, and A. M. Gemeay. Tangent exponential-G family of distributions with applications in medical and engineering, Alexandria Engineering Journal, 105(2024), 181–203.
- [28] S. Pu, T. Moakofi, and B. Oluyede. The Ristić-Balakrishnan-Topp-Leone-Gompertz-G family of distributions with applications, Journal of Statistical Theory and Applications, 22(2023), 116–150.
- [29] T. Moakofi and B. Oluyede. The Harris-Topp-Leone-G family of distributions: properties and applications, International Journal of Mathematics in Operational Research, 25(2)(2023), 208–241.
- [30] A. M. Gemeay, W. H. Alharbi, and A. R. El-Alosey. A new power G-family of distributions: properties, estimation, and applications, PLoS ONE, 19(8)(2024), e0308094.
- [31] M. Gabanakgosi and M. Otlaadisa. A new family of generalized-G distributions with properties and applications, Scientific African, 26(2024), e02344.
- [32] O. H. Odhah, H. M. Alshanbari, Z. Ahmad, F. Khan, and A. H. El-Bagoury. A new family of distributions using a trigonometric function: properties and applications in the healthcare sector, Heliyon, 10(9)(2024), e29861.
- [33] S. O. Bashiru, A. M. Isa, A. A. Khalaf, M. A. Khaleel, K. C. Arum, and C. L. Anioke. A hybrid cosine inverse Lomax-G family of distributions with applications in medical and engineering data, Nigerian Journal of Technological Development, 22(1)(2025), 261–278.
- [34] S. O. Bashiru, A. M. Isa, and I. Ali. Cosine Gompertz distribution: properties, simulation and application to Covid-19 and reliability engineering datasets, Confluence University Journal of Science and Technology, 1(2)(2024), 42–52. doi:10.5455/CUJOSTECH.241013.

SULE OMEIZA BASHIRU

DEPARTMENT OF MATHEMATICS AND STATISTICS, CONFLUENCE UNIVERSITY OF SCIENCE AND TECHNOLOGY, OSARA, KOGI STATE, NIGERIA.

ORCID: 0000-0002-6442-3286

Email address: bash0140@gmail.com

THATAYAONE MOAKOFI

INDEPENDENT RESEARCHER, PALAPYE, BOTSWANA.

ORCID: 0000-0002-2676-7694

 ${\it Email address:} \verb| thatayaone.moakofi@gmail.com|\\$